

## The influence of copolymerization with methacrylic acid on poly(butyl acrylate) film properties

Andrew Y.C. Koh<sup>a</sup>, Siyabonga Mange<sup>a</sup>, Marc Bothe<sup>b</sup>, Reinhold J. Leyrer<sup>b</sup>, Robert G. Gilbert<sup>a,\*</sup>

<sup>a</sup> School of Chemistry F11, Key Centre for Polymer Colloids, The University of Sydney, Sydney, NSW 2006, Australia

<sup>b</sup> BASF Aktiengesellschaft, GKD/A-B001, D-67056 Ludwigshafen, Germany

Received 1 November 2005; received in revised form 8 December 2005; accepted 14 December 2005

Available online 9 January 2006

### Abstract

The effects of methacrylic acid (MAA) on the physical properties of polymer made by emulsion copolymerization of butyl acrylate (BA) and MAA were examined. Emulsion polymerizations were performed with and without MAA and at temperatures of 0.1 and 50 °C, using redox initiation so that the radical flux was essentially independent of temperature. The presence of methacrylic acid had only a small effect on gel fraction and on molecular weight, but a profound effect on the film properties; changing the synthesis temperature was found to slightly alter the properties of the copolymer films. Latexes containing MAA formed much stronger films (from creep tests), and significantly increased tack and peel adhesion. This was attributed to intermolecular dipole–dipole interactions of the acid groups. Conductometric titration measurements revealed that the acid groups were predominantly located inside the latex particles, with only a small proportion in the aqueous phase and on the particle surface. Temperature was found not to affect significantly the partitioning of the acid groups in the latex.

© 2005 Elsevier Ltd. All rights reserved.

**Keywords:** Emulsion copolymerization; Butyl acrylate; Methacrylic acid

### 1. Introduction

Pressure sensitive adhesives (PSAs) are highly viscous and viscoelastic liquids which stick to a wide variety of surfaces when pressed down gently, and are used as ‘easy to apply’ self-adhesive products, e.g. labels and tapes. Extensive employment of acrylates as PSAs only began in the 1950s, although acrylate polymers have been known for a long time and were recognized as suitable PSA candidates as early as 1933 [1]. As only a few acrylate polymers are inherently pressure-sensitive, monomers are usually copolymerized to alter the physical and chemical properties of the PSA to meet application requirements. The synthesis is usually carried out by emulsion polymerization [2].

Functional groups are usually incorporated into latexes by copolymerization with comonomers such as acrylic and methacrylic acids, which are both water-soluble. These can have two effects: (a) they may impart colloidal stability to the latex through the formation of electrosteric stabilizers, as

a ‘hairy layer’ which is anchored to the particle by subsequent polymerization with hydrophobic monomer, i.e. the formation of a blocky copolymer. The hydrophilic component of this blocky copolymer is largely (meth)acrylic acid with a small amount of the hydrophobic monomer; (b) there may be incorporation of the acid within the particle, leading to formation of a random copolymer in the interior of the latex particle, comprising largely the hydrophobic monomer with a small amount of (meth)acrylic acid. At concentrations as low as 5 wt% and less, these comonomers are able to impart very significant improvements in properties such as peel strength and tensile strength.

Some of the factors that influence the distribution of the acid in latexes are: (a) the pH dependence of the partitioning [3]; (b) the reactivity ratios for copolymerization; (c) the physical state of the particles at the polymerization temperature; and (d) the process used (batch or semi-batch [4]). Ding et al. [5] found that in their carboxylated poly(butyl methacrylate-co-butyl acrylate) latex, most of the methacrylic acid (MAA) was buried in the particles and only a small amount was present in the aqueous phase. They showed that increasing the MAA concentration increased and decreased the acid distribution on the particle surface and aqueous phase, respectively. Santos and co-workers [3] showed that under typical emulsion polymerization conditions, the partition coefficients of styrene

\* Corresponding author. Tel.: +61 2 9351 3366; fax: +61 2 9351 8651.

E-mail address: [gilbert@chem.usyd.edu.au](mailto:gilbert@chem.usyd.edu.au) (R.G. Gilbert).

and butyl acrylate (BA) were highly dependent on temperature, but not affected by pH or relative concentration of organic material in the system. In contrast, the partition coefficient of MAA was independent of temperature but was strongly affected by pH, with the partition coefficient decreasing as the pH was increased from 2 to 6. Increasing the pH further led to a complete dissolution of the acid in the aqueous phase. The authors attributed this behaviour to the ionized carboxylic groups having a greater affinity for water.

This work investigates the effect of MAA on the properties of films obtained from emulsion copolymerization of BA, the commonest base for PSAs. The objective is to understand the effects that the presence of MAA has on both structure and physical properties of the formed film. The structural parameters examined are gel fraction, molecular weight, location of the MAA and branching fraction. The physical properties examined are the viscoelastic behaviour of the formed film, creep (strain as a function of time under stress), glass transition temperature ( $T_g$ ), tack and adhesive strength. Because of the effect of temperature on partitioning observed by Santos et al. [3], and because many of the rate coefficients governing the process have significant activation energies (e.g. that for BA propagation is  $18 \text{ kJ mol}^{-1}$  [6,7]), the synthesis was performed over a wide temperature range (0 and  $50 \text{ }^\circ\text{C}$ ); a redox initiation system was used to ensure that the radical flux was not strongly dependent on temperature.

## 2. Experimental

### 2.1. Materials

Butyl acrylate (BA, >99%) and methacrylic acid (MAA, 99%), purchased from Aldrich, were de-inhibited with a column packed with a methyl-hydroquinone inhibitor remover and used immediately. *t*-Butyl hydroperoxide (5%), sodium dodecyl sulfate (SDS), sodium metabisulfite (97%) and sodium hydroxide were obtained from Aldrich and used as received. Iron(III) sodium EDTA (Akzo Nobel, 40%) and a 20–50 mesh Bio-Rad mixed bed ionic resin were used as received.

### 2.2. Emulsion (co)polymerization

The (co)polymers were synthesized by emulsion copolymerization in a Mettler RC1e reactor. The initial charge in the reactor comprised water (181 g) containing iron(III) sodium EDTA (0.23 g), 4.3 g  $\text{Na}_2\text{S}_2\text{O}_5$  and 2.9 g acetone (which accelerates the redox initiation reaction—e.g. [8]), plus 48 g of the *t*-butyl hydroperoxide; this initial charge was allowed to thermally equilibrate. The monomer feed (comprising 172 g water, 32 g 30% SDS solution, 7.7 g 25% NaOH solution, 9.8 g methacrylic acid and 470 g of BA) and the rest of the redox initiator (a further 48 g *t*-butyl hydroperoxide) were fed into the reactor via two pumps. Initially, 10% of the monomer was fed in, and then controlled feed of the monomer and initiator continued to completion. Sample code BA/MAA0.1 corresponds to the emulsion copolymerization of BA and MAA at  $0.1 \text{ }^\circ\text{C}$ . For samples BA0.1 and BA50 (the 0.1 and 50 indicating

the polymerization temperature), MAA was replaced with an equimolar amount of SDS. The exotherm measured during the reactions did not exceed  $0.5 \text{ }^\circ\text{C}$ .

### 2.3. Characterization

$^{13}\text{C}$  NMR scans for BA/MAA0.1 dissolved in  $\text{CDCl}_3$  were recorded in solution at  $37 \text{ }^\circ\text{C}$  on a Varian spectrometer operating at 500 MHz.

The molecular weight distribution of the polymers was determined by analysis on a Waters size exclusion chromatography (SEC) system with a 510 HPLC pump, with a mixed-bed Styragel/HT 6E column and high-purity tetrahydrofuran (THF, Unichrom) eluent with a flow rate of  $0.8 \text{ mL min}^{-1}$ . The detector system used was an R401 differential refractometer. The polymer solutions for the SEC analysis were made to 1 wt% poly(BA) in THF.

The weight average molecular weight data from SEC,  $\bar{M}_w$  (SEC), were compared to the values  $\bar{M}_w$  (MALLS) obtained from a Zimm plot obtained by multi-angle laser light scattering (MALLS). The MALLS measurements were performed on the DAWN<sup>®</sup> EOS<sup>™</sup> Enhanced optical system configured in batch mode. A drop of the polymer latex was diluted with THF and five samples within a concentration range of  $4 \times 10^{-5}$ – $7 \times 10^{-3} \text{ g mL}^{-1}$  were prepared in 20 mL scintillation vials. Filtered toluene was used as the calibration solvent, pure THF was used to establish the baseline and a polystyrene standard with a number average molecular weight of 15,000 in THF was used as a reference. For the MALLS measurements, the differential index of refraction,  $dn/dc$ , was found to be  $0.0565 \text{ mL g}^{-1}$  for poly(BA) in THF at  $25 \text{ }^\circ\text{C}$  ( $\lambda = 690 \text{ nm}$ ). The gel content of the polymers was determined by ultracentrifugation [9] of a 1 wt% polymer solution in toluene at 12,000 rpm for 2 h to separate the soluble and insoluble fractions, followed by drying and weighing of the fractions.

The  $T_g$  of the polymer films was determined using a differential scanning calorimeter (TA Instruments 2920 modulated DSC). About 15 mg of polymer was accurately weighed in aluminium DSC pans, crimped and subjected to a modulating heating program of  $7 \text{ }^\circ\text{C min}^{-1}$  along with an empty reference pan in a DSC furnace.

The distribution of the MAA in the latex was determined by conductometric titration [5,10]. The aqueous phase was separated from the latex particles by ultracentrifugation of the latex at 90,000 rpm for 30 min at  $5 \text{ }^\circ\text{C}$  in a Beckman Coulter Optima L-100 XP Ultracentrifuge. Using the Malvern Instruments MPT-2 multi purpose titrator, the aqueous solution was then titrated against a 0.101 M NaOH solution to give the amount of acid in the aqueous phase. The amount of acid on the particle surface was determined by titrating a diluted latex solution against a 0.039 M NaOH. This sample was obtained by diluting the parent latex to 5 wt% solids and removing the free ions with a Bio-Rad mixed ion exchange resin until a conductivity less than  $8 \text{ } \mu\text{S}$  was achieved. The amount of acid inside the particle was then determined by mass balance.

The tensile viscoelastic and creep behaviour of the samples were measured using a TA Instruments DMA 2980 dynamic

mechanical analyzer fitted with a shear sandwich clamp. Films (10 mm<sup>2</sup> and 0.5–2 mm thick) were prepared by drying the latexes on Teflon<sup>®</sup> blocks at room temperature for 5 days. For each sample, two equal size films were aligned and mounted between a fixed outer plate and a moving centre plate on the DMA instrument. The DMA was operated under controlled force (stress) with a single oscillation frequency of 1 Hz to monitor the stress/strain behaviour of the films. The creep behaviour was evaluated by observing the film elongation as a function of time under a fixed load (1 N).

The adhesive properties of the polymers were obtained [11] by casting films on a Mylar sheet substrate to a thickness of about 22 g m<sup>-2</sup> and drying in an oven at 90 °C for 3 min. The viscosity of all latexes was adjusted with 0.1–0.2% Collacral PU85 thickener. The peel adhesion test involves measuring the force required to remove a pressure-sensitive adhesive from a plate. The standard peel adhesion used here is to Afera steel, and was measured by allowing the coated Mylar sheet to stand for 20 min, followed by passing over a 2 kg weight twice, then leaving for 20 min before measuring the force required to peel off at an angle of 180° at a speed of 300 mm min<sup>-1</sup>. The loop-tack to Afera steel test was done by raising the Afera steel panel to a Mylar coated loop, keeping in contact for 7 s and then removing at a crosshead speed of 300 mm min<sup>-1</sup>.

### 3. Results and discussion

Emulsion polymerization data and latex characteristics are summarized in Table 1.

#### 3.1. Branching fraction

During the free-radical polymerization of BA, long- and short-chain branching arise, respectively, from intermolecular and intramolecular (backbiting) radical transfer to polymer. The ratio of long- to short-chain branching cannot be accurately quantified using current characterization techniques without recourse to model-based assumptions. It is thought that backbiting is the dominant reaction at the temperatures used here [12]. Intermolecular chain transfer to polymer followed by bimolecular termination by combination leads to gel formation in poly(BA) (cross-linking). Former et al. [9] found no clear relationship between the gel fraction and the degree of branching for a pure poly(BA) system.

A representative solution-state <sup>13</sup>C NMR spectrum of the copolymer is shown in Fig. 1. The assignments of the peaks are based on those in the literature [12–15]. The level of branching of the copolymer was based on the proportion of the quaternary

carbon,  $C_h$ , to half the total integral for backbone carbon atoms [13,15]:

$$\text{Fraction branches} = \frac{C_h}{C_h + (C_{d+e+f}/2)} \quad (1)$$

where  $C_h$  is the area of the peak  $h$  in Fig. 1. Based on the integration of the peaks (Table 2) of interest from Fig. 1 and utilizing Eq. (1), the amount of branching in the sample synthesized at 0.1 °C was found to be 0.5%. As noted, this gives the total amount of branches present and does not distinguish between long-chain and short-chain branches. The amount of branching in the polymer is similar to that observed by Plessis et al. [12] for their poly(BA) produced in pulsed-laser polymerization experiments, i.e. ca. 0.316% branches for a monomer concentration,  $[M_0]=2.48$  M at  $-1$  °C. Because this branching is predominantly short-chain and thus intra-chain, the amount of branching will not depend on conversion. This suggests that the presence of the small amount of MAA used here (2%) does not have a significant effect on the total branching.

#### 3.2. Molecular weight analysis

Former et al. [9] examined the recovery of poly(BA) after SEC and showed that significant amounts of polymer did not reach the SEC detector, probably because of the presence of microgel in poly(BA). This implies that SEC is not able to analyze the true polymer molecular weight distribution for this system. This issue is addressed in the present paper by measuring the  $\bar{M}_w$  of the polymer using MALLS, without passing through an SEC column.

Molecular weight data of the samples determined by SEC are given in Table 3. Also shown are the  $\bar{M}_w$  values using Zimm plots from MALLS, as shown in Fig. 2. The MALLS values for  $\bar{M}_w$  are much higher than those obtained from SEC measurements. This is probably a manifestation of high molecular weight species trapped in the guard column (prefilter) prior to entering the SEC columns. It was also found that the samples for SEC were difficult to filter and exhibited weak signals. Again, this suggests that some of the sample was lost during the filtration step. These observations, coupled with the strong curvature of the Zimm plots, suggest that the copolymer, and also poly(BA) homopolymer, can be classified into gel and soluble fractions and also into an intermediate fraction which comprises microgels, as suggested by Former et al. [9].

In a separate experiment, the viscosity-average molecular weight,  $\bar{M}_v$ , of a poly(BA) sample prepared at 0 °C was obtained from viscometry. The data are expressed as a dual Huggins–Kraemer plot in Fig. 3 to yield the intrinsic viscosity  $[\eta]$ . Using the Mark–Houwink parameters [16]  $K=12.2 \times 10^{-5}$  dL g<sup>-1</sup> and  $a=0.7$  with the value of  $[\eta]=9.82$  dL g<sup>-1</sup> determined from the viscometry measurements gives  $\bar{M}_v=10 \times 10^6$ . This value is comparable to the  $\bar{M}_w$  determined by MALLS ( $6.7 \times 10^6$ ).

The gel content data (shown in Table 1) from ultracentrifugation measurements indicate that BA/MAA0.1 contains

Table 1  
Emulsion copolymerization data and latex characteristics

Sample	Conversion (%)	Solids content (%)	Gel content (%)	$T_g$ (°C)
BA/MAA0.1	95	45	17	-46.96
BA/MAA50	95	41		
BA0.1	95	50	15	-44.98
BA50	90	40		

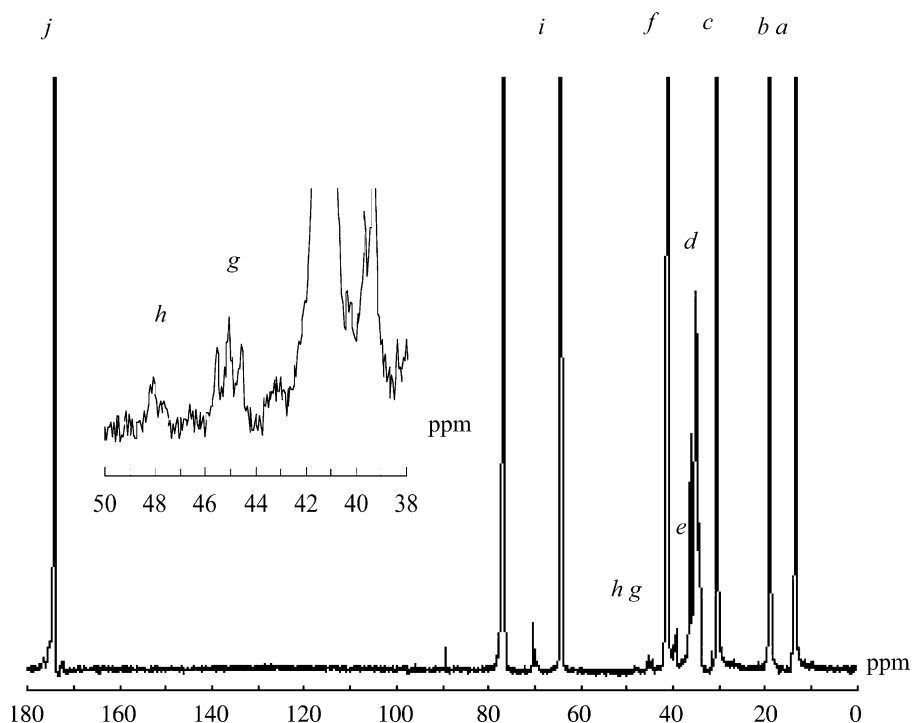


Fig. 1. Solution-state  $^{13}\text{C}$  NMR of the copolymer in  $\text{CDCl}_3$  measured at  $37^\circ\text{C}$ . The assignments of the peaks are tabulated in Table 2. The inset shows peaks  $g$  and  $h$ , which corresponds to the branch points of poly(MAA) and poly(BA), respectively.

17% gel. Thus, there is no direct relationship between the gel content and % branches. Importantly, the gel content was found to be strongly dependent on the dissolution period (data not shown). The decrease in gel content with time was attributed to polymer chains dissolving slowly, followed by branched chains and finally true gels, i.e. longer and/or branched chains take much longer time to dissolve.

It is likely that some of the gel in MAA/BA copolymerization arises from the same process as in the homopolymerization of BA, viz. the intermolecular chain transfer to polymer followed by bimolecular termination by combination. Chain transfer to monomer which produces terminal double bonds, leading to the possibility of gel formation by intermolecular

chain transfer to polymer and propagation to the terminal double bonds, might also be significant in the present system.

The addition of MAA causes a small decrease in  $\bar{M}_w$  compared to that of BA homopolymer, which can be ascribed to a number of causes in the complex relations between copolymerization rate parameters and molecular weight. This change is insufficient to have a significant effect on physical properties in its own right.

### 3.3. Differential scanning calorimetry

The  $T_g$  values of poly(BA) and that of poly(BA-co-MAA), given in Table 1, are similar. These values can be compared with the prediction from the Pochan equation [17] for random copolymers, which in the present case is:

$$\ln T_g = (m_{\text{BA}} \ln T_{g\text{BA}} + m_{\text{MAA}} \ln T_{g\text{MAA}}) \quad (2)$$

with  $m_{\text{BA}}$  and  $m_{\text{MAA}}$  the weight fractions of BA and MAA in feed, respectively.  $T_{g\text{BA}}$  and  $T_{g\text{MAA}}$  are the glass transition temperatures for poly(BA) ( $-43^\circ\text{C}$  [18]) and poly(MAA) ( $162^\circ\text{C}$  [19]). This predicts an increase in  $3^\circ\text{C}$  in the  $T_g$  of poly(BA) from  $-43$  to  $-40^\circ\text{C}$  when 2 wt% MAA is added. The present data in fact

Table 2  
Assignments of the  $^{13}\text{C}$  NMR spectrum (Fig. 1) of poly(BA-co-MAA) in  $\text{CDCl}_3$

Peak	Chemical shift (ppm)	Assignment
<i>a</i>	14	$\text{CH}_3$ in butyl side group
<i>b</i>	19	$\text{CH}_2$ in butyl side group and $\alpha\text{-CH}_3$ of poly(MAA)
<i>c</i>	31	$\text{CH}_2$ in butyl side group
<i>d</i>	35	Main-chain $\text{CH}_2$ of poly(BA) and poly(MAA)
<i>e</i>	39	$\text{CH}_2$ of poly(BA) next to branch point
<i>f</i>	41	Main-chain CH of poly(BA)
<i>g</i>	44	Branch point of poly(MAA)
<i>h</i>	48	Branch point of poly(BA)
<i>i</i>	64	$\text{CH}_2$ next to ester group in poly(BA)
<i>j</i>	175	Carbonyl group of poly(BA) and poly(MAA)

Note that only major peaks in the spectrum are assigned.

Table 3  
Molecular weight data from SEC and MALLS

Sample	From SEC		From MALLS
	$\bar{M}_w/10^6$	Polydispersity	$\bar{M}_w/10^6$
BA/MAA0.1	0.37	4.1	5.6
BA/MAA50	0.39	5.7	
BA0.1	0.46	4.1	6.7



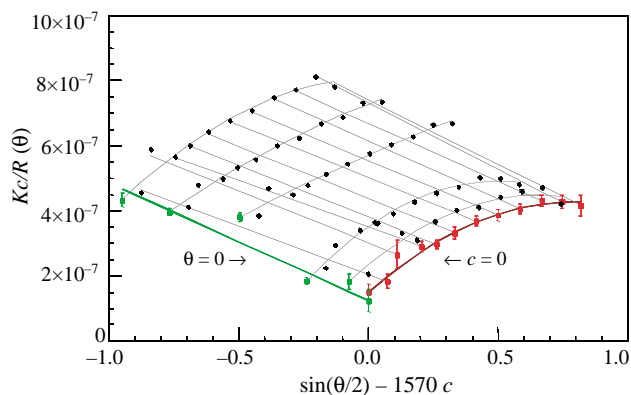


Fig. 2. Zimm plot for BA/MAA0.1 constructed from MALLS measurements.

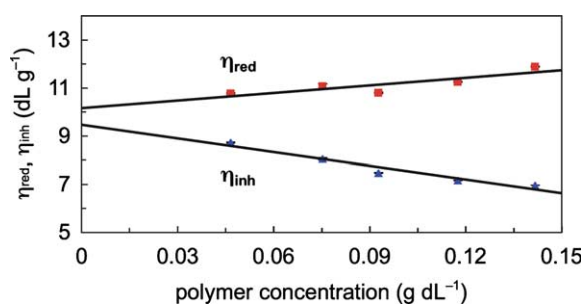


Fig. 3. Reduced and inherent viscosities as a function of polymer concentration (Huggins–Kraemer plot) used to obtain intrinsic viscosity for BA latex prepared at 0.1 °C.

show a slight (2 °C) decrease in  $T_g$ . This may be due to the presence of the hydrophilic monomer slightly increasing the water content of the film, with the water acting as a plasticizer, an effect well known in, for example, poly(vinyl acetate) (e.g. [20]).

### 3.4. Acid distribution in latexes

The results obtained from conductometric titration measurements are shown in Table 4. The data reveal that most of the acid resides inside the particle and that different synthesis temperatures have little influence on the distribution. This behaviour has been noted by Santos et al. [3], who found that partitioning of MAA at temperatures of 25 and 70 °C was influenced more by pH rather than temperature. In our work, the reaction mixture prior to addition of the feed had a pH of 1.9. At this pH MAA is in its non-dissociated form, which is less polar than the dissociated form found at higher pH values. The former partitions preferentially in the organic phase, i.e. inside the particles. The data suggest that there are very low

Table 4  
Amounts of acid groups of the latexes containing MAA from conductometric titration

Sample	COOH ( $10^{-5}$ mol)/latex polymer (g)	
	BA/MAA0.1	BA/MAA50
Aqueous phase	2.58	0.32
Particle surface	1.11	0.37
Buried inside particle	23.25	27.73

levels of MAA in the aqueous phase [21] and on the particle surface, and that MAA does not play a significant role as an electrosteric stabilizer. Its main effect is to change the bulk viscoelastic properties of the films (see below) [22].

The NMR data can be used to check this inference by considering the amount of MAA present within the film. The peak at  $\delta=45$  ppm corresponds to the quaternary carbon of poly(MAA). Comparing the area of this peak to the total area for the polymer gives an area of ca. 2.0%. This is comparable to the amount of acid in the recipe of ca. 2.0%, supporting the inference that most of the MAA is inside the particles under these reaction conditions.

### 3.5. Dynamic mechanical analysis

Fig. 4 shows the stress vs. strain plots for the samples measured using DMA. The straight line at low stress values corresponds to the linear viscoelastic region of the sample. As can be seen from the plots, poly(BA-co-MAA) exhibits a larger viscoelastic range ( $\leq 15\%$  strain) compared to poly(BA) ( $\leq 5\%$  strain). As will be explained in more detail later, the presence of MAA results in intermolecular dipole–dipole interactions of the acid groups [23]. Chan and Howard [24] attributed these interactions as being responsible for the observed improved film adhesion at low concentration of acid. However, they found the tack to decrease with increasing acid concentration, as a result of hardening of the film. According to these authors, these observations are not specific to poly(BA) containing MAA, as similar behaviour was observed for the copolymerization of ethyl acrylate and acrylonitrile.

The effect of MAA on the mechanical properties of the copolymers can be also observed from the creep measurements (Fig. 5). The plot shows that for a given extension, additional time is required for the copolymer to elongate compared to the homopolymer. Mechanical strength in copolymer films arises by the interdiffusion of copolymer chain ends and segments and the formation of chain entanglements across the latex particle boundaries [25]. The dipole–dipole interactions of the acid groups in the MAA copolymer retard the copolymer

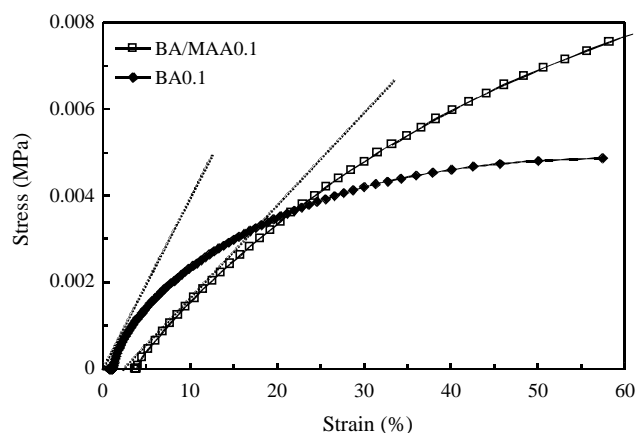


Fig. 4. Stress vs. strain plots for the copolymer films measured by DMA at 1 Hz. The straight line corresponds to the linear viscoelastic region.

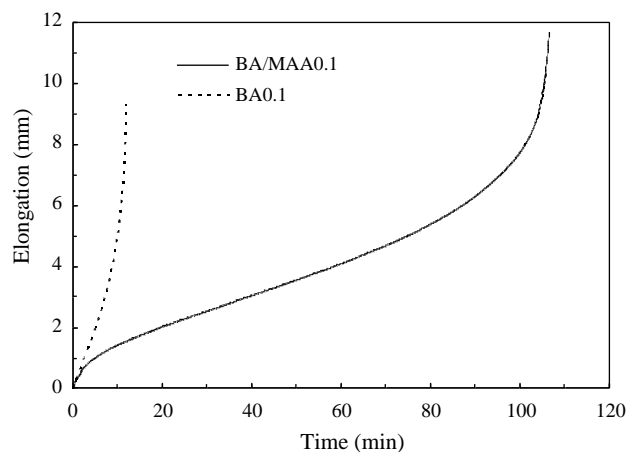


Fig. 5. Elongation as a function of time for the copolymer samples as determined from the creep experiment.

chains from moving/slipping past one another in the presence of a load, thus increasing the time it takes to elongate compared to a BA homopolymer.

The adhesive performance of the films was quantified by the tack (ability of the material to stick quickly to a substrate) and adhesion properties (how strongly the material adheres to substrate). The results obtained from loop tack and peel adhesion experiments are listed in Table 5. The data show that in the presence of MAA the film is tackier and more adhesive compared to poly(BA). This can be attributed to the increased cohesive and adhesive strength of poly(BA-*co*-MAA) compared to poly(BA) as a result of intermolecular dipole–dipole interactions in the acid groups in BA/MAA0.1. It can be seen from Table 5 that at high pH (BA/MAA0.1/8.15) the tack and film adhesion is lower compared to BA/MAA0.1, i.e. the sample with unadjusted pH. As the pH of BA/MAA0.1, pH = 8.15, is significantly greater than the pK<sub>a</sub> of MAA [26] of 4.65, the MAA groups can be considered to be completely ionized. On the other hand, the unadjusted sample (pH = 4.98) has only 68% of ionized MAA. Thus, there is a high concentration of

Table 5  
Film performance as determined from loop tack and peel adhesion measurements

Sample	Loop tack		Peel adhesion	
	F (N)	Comments <sup>a</sup>	F (N)	Comments <sup>a</sup>
BA/MAA0.1	11.06	AF with some AT and AS	8.92	CF
BA/MAA0.1/8.15 <sup>b</sup>	4.81	Complete AT	1.77	AF with some AT
BA/MAA50	4.59	AF	3.67	75% AT, 25% AF
BA0.1	1.60	AF with some AT	2.84	AF with some AT

Film width = 25 mm. F = force. Test methods based on the international reference standard for self-adhesive materials [11].

<sup>a</sup> AF, adhesive failure: the adhesive fails to stick with the substrate; AT, adhesive transfer: the adhesive separates cleanly from the material leaving adhesive on the substrate; AS, adhesive stain: leaves adhesive impression where it comes in contact with the substrate; CF, cohesive failure: the adhesive film splits during test, leaving residue on both the substrate and the material.

<sup>b</sup> The latex is essentially similar to BA/MAA0.1 except that the pH of the sample was brought to 8.15 prior to coating the sample on a Mylar sheet.

dipole–dipole interactions of the protonated acid species in BA/MAA0.1, leading to a greater tack and film adhesion.

The strong dependence of the peel adhesion on the viscoelastic response of the films is evident by comparison of the stress vs. strain plots (Fig. 4) to the peel adhesion data (Table 5) for samples BA/MAA0.1 and BA0.1. It is apparent that the adhesive strength is directly related to the viscoelastic nature of the film [22]. Briefly, as the peel rate increases the viscoelastic response changes from viscous through rubbery to glassy. As a result, the peeling behaviour changes from cohesive separation through adhesive separation and finally to extremely low peel force. The greater peel adhesion of BA/MAA0.1 is a manifestation of the sample exhibiting greater viscous and rubbery behaviour due to its wider viscoelastic range compared to BA0.1. Again, this is due to the presence of carboxylic acid groups in BA/MAA0.1. It should be noted that the rubbery response is considered most pertinent since the separation between adhesive and substrate usually involves this mode of peeling.

The slight dependence of mechanical properties on temperature can be explained as follows. The  $\bar{M}_w$  of BA/MAA50 will be lower than that of BA/MAA0.1, since transfer to monomer (which is a major chain-stopping event in BA) has a relatively high activation energy [27]. As the mechanical strength in copolymer films arises by the interdiffusion of copolymer chain ends and segments and the formation of chain entanglements, it follows that BA/MAA50 with its shorter chains will exhibit lower tack and peel adhesive (related to viscoelastic) behaviour compared to BA/MAA0.1.

#### 4. Conclusions

Homopolymerization and copolymerization of BA with small amounts of MAA were carried out at 0.1 and 50 °C. Mechanical analysis showed that the copolymerization of BA with small amounts of MAA enhanced the tensile and adhesive properties of poly(BA-*co*-MAA) compared to those of poly(BA). The change in film properties were attributed to the intermolecular dipole–dipole interactions when a polar comonomer, i.e. MAA, was present.

There was a slight difference in the adhesive properties of poly(BA-*co*-MAA) at the two polymerization temperatures. Conductometric titration experiments showed that the distribution of the MAA in the latexes was similar at both polymerization temperatures and found to be predominantly inside the particles.

#### Acknowledgements

We gratefully acknowledge the support of the Australian Research Council's Linkage program, and financial support of BASF AG, as well as stimulating discussions with Dr Brad Morrison of that company, and with Dr David Lamb of the KCPC. The collaboration of Dr Marianne Gaborieau in the NMR measurements is greatly appreciated, and of Donna O'Shea (BASF Australia) for carrying out the tack and peel

tests. The Key Centre for Polymer Colloids was established and supported under the ARC's Research Centres Program.

## References

- [1] Bauer W. German Patent DE575327; 1933.
- [2] Urban D, Takamura K. Polymer dispersions and their industrial applications. Weinheim: Wiley–VCH; 2002.
- [3] Santos AM, Guillot J, McKenna TF. Chem Eng Sci 1998;53:2143.
- [4] Lovell PA. In: Lovell PA, El-Aasser MS, editors. Emulsion polymerization and emulsion polymers. Chichester: Wiley; 1997.
- [5] Ding TH, Daniels ES, El-Aasser MS, Klein A. J Appl Polym Sci 2005;97:248.
- [6] Lyons RA, Hutovic J, Piton MC, Christie DI, Clay PA, Manders BG, et al. Macromolecules 1996;29:1918.
- [7] Asua JM, Beuermann S, Buback M, Charleux B, Gilbert RG, Hutchinson RA, et al. Macromol Chem Phys 2004;205:2151.
- [8] Shaffei KA, Ayoub MMH, Ismail MN, Badran AS. Eur Polym J 1998;34:553.
- [9] Former C, Castro J, Fellows CM, Tanner RI, Gilbert RG. J Polym Sci, Part A: Polym Chem Ed 2002;40:3335.
- [10] Tang JS, Ding TH, Daniels ES, Dimonie VL, Klein A, El-Aasser MS. J Appl Polym Sci 2003;88:30.
- [11] FINAT technical handbook. The Hague; 2001.
- [12] Plessis C, Arzamendi G, Alberdi JM, van Herk AM, Leiza JR, Asua JM. Macromol Rapid Commun 2003;24:173.
- [13] Ahmad NM, Heatley F, Lovell PA. Macromolecules 1998;31:2822.
- [14] Johnson DE, Lyerla JR, Horikawa TT, Pederson LA. Anal Chem 1977;49:77.
- [15] Plessis C, Arzamendi G, Leiza JR, Schoonbrood HAS, Charmot D, Asua JM. Macromolecules 2000;33:5041.
- [16] Beuermann S, Paquet DA, McMinn JH, Hutchinson RA. Macromolecules 1996;29:4206.
- [17] Pochan JM, Beatty CL, Pochan DF. Polymer 1979;20:879.
- [18] Penzel E, Rieger J, Schneider HA. Polymer 1997;38:325.
- [19] Penzel E. In: Penzel E, editor. Ullman's encyclopedia of industrial chemistry. Weinheim: Wiley–VCH Verlag GmbH and Co. KGaA; 2000.
- [20] Royal JS, Torkelson JM. Macromolecules 1992;25:1705.
- [21] Chern CS, Lin FY, Chen YC, Lin CH. J Appl Polym Sci 1996;62:585.
- [22] Aubrey DW, Ginosatis S. J Adhes 1981;12:189.
- [23] Dhal PK, Deshpande A, Babu GN. Polymer 1982;23:937.
- [24] Chan H-K, Howard GJ. J Adhes 1978;9:279.
- [25] Voyutskii SS, Ustinova ZM. J Adhes 1977;9:39.
- [26] Diez-Pena E, Quijada-Garrido I, Frutos P, Barrales-Rienda JM. Polym Int 2003;52:956.
- [27] Maeder S, Gilbert RG. Macromolecules 1998;31:4410.